Progress in Neuropsychopharmacology & Biological Psychiatry 134 (2024) 111065

Contents lists available at ScienceDirect

Progress in Neuropsychopharmacology & Biological Psychiatry

journal homepage: www.elsevier.com/locate/pnp

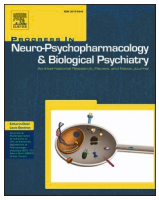

Developmental activity-based anorexia alters hippocampal non-genomic stress response and induces structural instability and spatial memory impairment in female rats

Francesca Mottarlini [a,1], Giorgia Targa [a,1], Beatrice Rizzi [a,b], Fabio Fumagalli [a], Lucia Caffino [a,*]

[a] Department of Pharmacological and Biomolecular Sciences 'Rodolfo Paoletti', Università degli Studi di Milano, Via Balzaretti 9, 20133 Milano, Italy
[b] Center for Neuroscience, University of Camerino, Camerino, Italy

ARTICLE INFO

Keywords:
Anorexia nervosa
Adolescence
Corticosterone
Glutamatergic synapse
Dendritic spine
Cognition
Hippocampus

ABSTRACT

Objective: Anorexia nervosa (AN) is characterized by hyperactivation of the hypothalamic-pituitary-adrenal axis and cognitive deficits. However, little is known about the rapid non-genomic stress response involvement. This study investigates the molecular, structural and behavioral signatures of the anorexic phenotype induction in female rats on stress-related mechanisms in the hippocampus.

Method: Female adolescent rats, exposed to the combination of food restriction and wheel access, i.e., the activity-based anorexia (ABA) protocol, were sacrificed in the acute phase of the pathology (postnatal day [P]42) or following a 7-day recovery period (P49).

Results: ABA rats, in addition to body weight loss and increased wheel activity, alter their pattern of activity over days, showing increased food anticipatory activity, a readout of their motivation to engage in intense physical activity. Corticosterone plasma levels were enhanced at P42 while reduced at P49 in ABA rats. In the membrane fraction of the hippocampus, we found reduced glucocorticoid receptor levels together with reduced expression of caldesmon, n-cadherin and neuroligin-1, molecular markers of cytoskeletal stability and glutamatergic homeostasis. Accordingly, structural analyses revealed reduced dendritic spine density, a reduced number of mushroom-shaped spines, together with an increased number of thin-shaped spines. These events are paralleled by impairment in spatial memory measured in the spatial order object recognition test. These effects persisted even when body weight of ABA rats was restored.

Discussion: Our findings indicate that ABA induction orchestrates hippocampal maladaptive structural and functional plasticity, contributing to cognitive deficits, providing a putative mechanism that could be targeted in AN patients.

1. Introduction

Anorexia nervosa (AN) is a multifaceted psychiatric disorder with an estimated lifetime prevalence of 4% among females and 0.3% among males (van Eeden et al., 2021), a mortality rate of 15.9% (Arcelus et al., 2011; Guinhut et al., 2021; Iwajomo et al., 2021) and a rapidly decreasing age of onset (Petkova et al., 2019; Holland et al., 2016). Its core symptoms are food avoidance and overexercise to fulfill the weight-loss desire (DSM-V., 2013). Despite the common belief that AN has a psychosocial origin with clear symptomatology, the triggers of the disorder and the relative biological implications underlying the elective starvation behaviors with hyperactive regimens are still elusive and the pharmacological treatments are ineffective (Zipfel et al., 2015).

Evidence exists that, in parallel to the maladaptive reorganization of the mesocorticolimbic structures in both AN patients and animal models (Mottarlini et al., 2020; Foldi et al., 2017; Frank et al., 2018; Mottarlini et al., 2022a; Chowdhury et al., 2014a; Ho et al., 2016), the hypothalamic-pituitary-adrenal (HPA) axis may play a role in the anorexic endophenotype (Bou Khalil et al., 2017). AN patients display a hyperactivation of the HPA axis (Monteleone et al., 2001), showing increased plasma cortisol, central corticotropin-releasing hormone and arginine vasopressin (Licinio et al., 1996; Walsh et al., 1987; Connan

* Corresponding author at: Department of Pharmacological and Biomolecular Sciences 'Rodolfo Paoletti', Università degli Studi di Milano, Via Balzaretti 9, 20133 Milano, Italy.
E-mail address: Lucia.Caffino@unimi.it (L. Caffino).
[1] Francesca Mottarlini and Giorgia Targa contributed equally to the manuscript and can be both considered first author

https://doi.org/10.1016/j.pnpbp.2024.111065
Received 3 March 2024; Received in revised form 18 May 2024; Accepted 17 June 2024
Available online 18 June 2024
0278-5846/© 2024 The Author(s). Published by Elsevier Inc. This is an open access article under the CC BY-NC-ND license (http://creativecommons.org/licenses/by-nc-nd/4.0/).

et al., 2007), features shared with other psychopathologies such as anxiety (Kische et al., 2021), depression (Zajkowska et al., 2022) and obsessive-compulsive disorders (Sousa-Lima et al., 2019). Even though these malnutrition-induced effects are reversed by weight recovery (Kaye et al., 1989), the abnormal activity of the HPA axis in the acute phase of the disorder may lead to persistent dysfunctions of brain functionality, contributing to neuroendocrine, behavioral and cognitive alterations sustaining the AN phenotype (Bou Khalil et al., 2017). In animal models, it has already been shown that food restriction-induced hyperactivity relies on corticosterone (CORT) fluctuations (Duclos et al., 2009).

Glucocorticoids (GCs), the primary molecular mediators of the stress response, are known to modulate hippocampal structural organization via rapid non-genomic stress response (McEwen et al., 2016; Swanson et al., 2013). The hippocampus (Hip), critically involved in learning and memory (Bird and Burgess, 2008), is highly sensitive to stress and GCs (Cole et al., 2022). In particular, chronic stress induces atrophy of apical dendrites and modulation of spine density and shape through intracellular mechanisms reorganizing the neuronal cytoskeleton (de Kloet et al., 2005; Leuner and Shors, 2013; Hall et al., 2015). Underweight AN patients are extremely responsive to stressful situations, as shown by reduced Hip volume (Collantoni et al., 2021) and dendritic branching are altered in the Hip of a rat model of AN (Chowdhury et al., 2014b), contributing to induce anxiety and cognitive deficits (Aoki et al., 2017; Lamanna et al., 2019). GCs exert their biological activity by binding the high-affinity mineralcorticoid receptor (MR), rapidly saturated under physiological conditions, or the lower-affinity glucocorticoid receptor (GR), promptly activated after a significant rise in circulating GCs, such as after stress exposure or at the circadian peak of GCs secretion (Mifsud and Reul, 2018; Meijer et al., 2019; Reul and de Kloet, 1985). After GCs-GR binding, GR localized in cellular membranes (mGR) can regulate different intracellular processes within seconds or minutes, exploiting their rapid non-genomic effect, such as regulating glutamate release and modulating synaptic structures such as dendritic spines (Arango-Lievano et al., 2019; Park et al., 2015).

To understand the potential correlation between elevated levels of cortisol and cognitive impairments in AN patients, a few hypotheses have been formulated (Seed et al., 2002); however, their precise relationship is still unknown. Taking this into account, we focused on the potential implication of mGRs and the related activation of GR-associated signaling pathway in regulating hippocampal neuroplastic processes, which might play a role in the AN pathophysiology by altering cognitive functions (Rose et al., 2014; Stedal et al., 2022).

For this purpose, we applied the activity-based anorexia (ABA) protocol, a well-accepted preclinical model mimicking the typical traits of the anorexic disorder, i.e., the combination of caloric restriction and voluntary running activity (Mottarlini et al., 2020; Mottarlini et al., 2022a; Mottarlini et al., 2022b; Carrera et al., 2014; Barbarich-Marsteller, 2013). Following the induction of the AN phenotype, we explored the involvement of the HPA axis by measuring CORT plasma levels and the levels of mGR and its downstream effector Caldesmon-1 (CaD1), a structural protein relevant in synaptic remodeling (Tanokashira et al., 2012), in the Hip of adolescent female ABA rats. Then, we evaluated possible alterations in synaptic vesicle exocytosis by measuring Synapsin1 (Syn1) activation, an index of synaptic vesicle trafficking and neurotransmitter release (Moschetta et al., 2022), and in the structural architecture of hippocampal synapses, by evaluating markers of the post-synaptic density integrity such as post-synaptic protein (PSD) 93 and PSD95 (Won et al., 2017) and two trans-synaptic adhesion molecules n-cadherin and neuroligin-1, which glue together pre- and post-synaptic terminals in an activity-dependent fashion (Sudhof, 2021). Moreover, since alterations of mGR might impact synaptic function and stability, we analyzed dendritic spines through structural and morphological analyses and the homeostasis of the glutamatergic synapse by measuring AMPA and NMDA receptor subunits. Lastly, to correlate the abovementioned changes with potential hippocampal function alterations, we exposed ABA animals to the spatial order object recognition (SOOR) test, a cognitively demanding test that allows the evaluation of the rodent's ability to cope with spatial orientation changes mainly dictated by a proper hippocampal activity (Barker and Warburton, 2011). Behavioral and molecular evaluations were performed at two time points: at PND42, which is representative of the acute phase of the AN phenotype (25% of weight loss combined with hyperactivity on the wheel), and at PND49, after a period of body weight recovery, to check for long-lasting alterations persisting despite weight recovery.

2. Materials and methods

2.1. Animals

Adolescent female Sprague-Dawley outbred rats were purchased from Charles River (Calco, Italy). After their arrival, at post-natal day (PND) 24, animals were housed in groups of four per cage under standard conditions of temperature (21 ± 1 °C) and humidity (50–60%) and exposed under a reversed light/dark cycle (light on/off: 10.30 pm/10.30 am) and left undisturbed for one week. Animals were fed with standard rat chow (ssniff Spezialdiäten GmbH, Soest, Germany) and tap water ad libitum. To reduce the "litter effects", a maximum of two female siblings were sorted out from each litter (Chapman and Stern, 1978).

All animal procedures were conducted at the Department of Pharmacological and Biomolecular Sciences at the University of Milan and carried out following the principles set out in the following laws, regulations, and policies governing the care and use of laboratory animals: Italian Governing Law (D.lgs 26/2014; Authorization n.19/2008-A issued March 6, 2008, by Ministry of Health); the NIH Guide for the Care and Use of Laboratory Animals (Ed. 2011) and EU directives and guidelines (EEC Council Directive 2010/63/UE). Authorization for animal use has been obtained from the Italian Ministry of Health (#898–2016-PR). All efforts were applied to reduce animal suffering and to minimize the number of animals used; for ethical reasons, activity-based anorexia (ABA) animals were not allowed to lose >25% of their initial body weight. Under our experimental conditions, no rats reported a weight loss higher than 25% of their initial body weight. The experiments have been reported in compliance with the ARRIVE guidelines.

2.2. Experimental paradigm

Experiments started upon rats arrival on postnatal day (PND)24 and were conducted as previously described and represented in Fig. 1A (Mottarlini et al., 2022a). Briefly, from PND24 to PND30, animals were housed in groups in standard home cages and left undisturbed to get accustomed to the reversed light/dark cycle. At PND30, rats started to be weighed daily and then, at PND35, animals were individually housed and indiscriminately divided as follows: control (CTRL) group: sedentary (no wheel access) + food ad libitum; food-restricted (FR) group: sedentary + food limited for 2 h/day; exercise (EXE) group: exposed to voluntary running activity in a mechanical wheel + food ad libitum; activity-based anorexia (ABA) group: exposed to voluntary running activity in a mechanical wheel + food restriction (food limited for 2 h/day). At PND38, food restriction began for FR and ABA rats: animals had full and free access to food for 2 h, while wheels were blocked to prevent rats from preferring running over food. At PND42, half of the animals were sacrificed by decapitation to perform molecular analysis and by perfusion to perform structural analyses in the acute phase of the anorexic phenotype. At the same time, the remaining group was transferred into regular cages with food ad libitum for 7 days (until PND49) to allow bodyweight recovery and then, at PND49, sacrificed by decapitation to perform molecular analysis and by perfusion to perform structural analysis. At both time points, animals have been sacrificed at the beginning of the dark cycle.

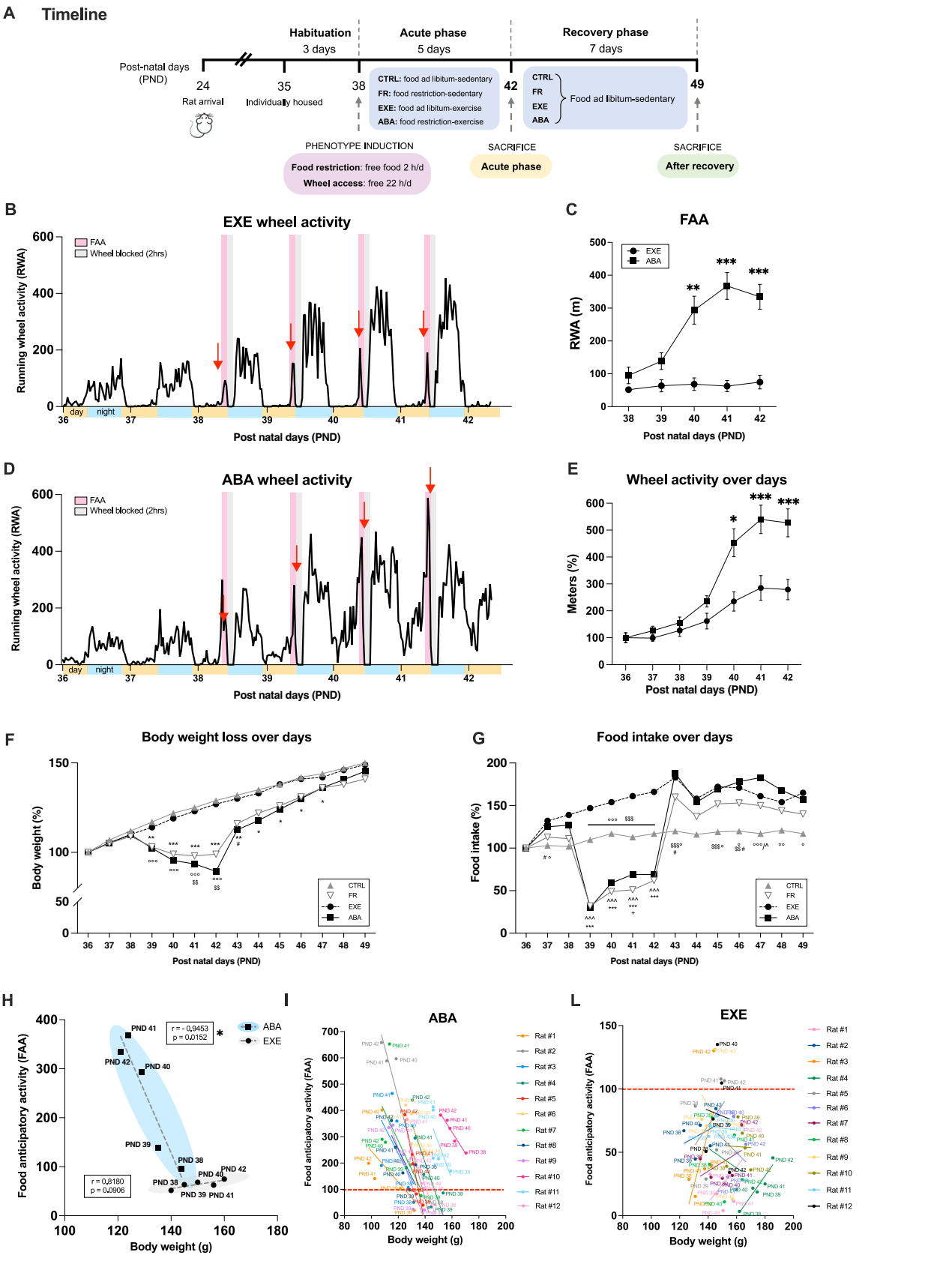

(caption on next page)

Fig. 1. Progression of running wheel activity (RWA) and body weight loss during the ABA protocol. Graphical representation of the experimental paradigm (A). Daily RWA evaluation for EXE (B) and ABA (D) rats during the active wheel period (PND 36-PND 42). The FAA calculated in the 2 h period prior the free food session is qualitatively represented in panel (B) and (D) highlighted in pink, peaks are indicated with red arrows, and it is quantitively represented in panel (C). Panel (E) shows the total wheel activity performed by EXE and ABA rats during the entire duration of the active wheel period. Daily body weight and food intake for CTRL, EXE, FR and ABA rats are shown in panel (F) and (G). Pearson's product-moment correlation (r) and linear regression analyses between body weight loss and FAA are represented as group mean for EXE (black dots) and ABA rats (black squares) during the acute phase of the ABA protocol (PND 38-PND 42) in panel (H) and as independent correlations for the ABA group in panel (I) and for the EXE group in panel (L). (For interpretation of the references to colour in this figure legend, the reader is referred to the web version of this article.)
Two-way ANOVA repeated measures followed by Sidak's multiple comparison test (RWA measurements panels C, E) $^{**}p < 0.01$, $^{***}p < 0.01$; followed by Tukey's multiple comparison test (Body weight measurement panel D; food intake measurement panel G) $^{***}p < 0.001$ FR vs EXE; $^{\$\$}p < 0.01$, $^{\$\$\$}p < 0.001$ vs FR; $^{\#}p < 0.01$ vs EXE; $^{\circ}p < 0.05$, $^{\circ\circ}p < 0.01$, $^{\circ\circ\circ}p < 0.001$ vs ABA; $^{\wedge}p < 0.05$, $^{\wedge\wedge\wedge}p < 0.001$ vs EXE and ABA; $^{+}p < 0.05$ FR vs ABA.
Pearson's product–moment correlation (r) analyses and linear regression analyses (R^2) between body weight and FAA (panel H).
CTRL: control ($n = 6$/time point); FR: food restriction ($n = 6$/time point); EXE: exercise ($n = 6$/time point); ABA: activity-based anorexia ($n = 6$/time point); FAA: food anticipatory activity period.

After decapitation, the Hip (defined as dorsal and ventral subregions) corresponding to plates 47–90 (−1.72 mm to −6.84 mm from Bregma) of the Paxinos and Watson atlas (Paxinos and Watson, 2013) was immediately dissected, frozen on dry ice and stored at −80 °C.

Three different sets of rats were used for molecular analysis (acute phase: CTRL, FR, EXE, ABA $n = 6$; recovery: CTRL, FR, EXE, ABA n = 6), for spine density and morphological studies (acute phase: CTRL, ABA $n = 4$; recovery: CTRL, ABA n = 4) and for spatial memory performance evaluation (acute phase: CTRL, ABA $n = 11$; recovery: CTRL, ABA n = 11).

2.3. Measurements

As previously described, bodyweight, food intake, and wheel-running activity were assessed per each animal daily at 9.30 am (Mottarlini et al., 2020). Rodent voluntary physical activity on the wheel was registered every 30 min through a counter device connected to the running wheel (activity wheel BIO-ACTIVW- R cage, Bioseb, France) and associated with recording software (BIO-ACTIVW-SOFT v1.2.1, Bioseb). The food anticipatory activity (FAA) was calculated for each rat as the distance in meters (m) traveled on the wheel during the 2 h before the feeding time.

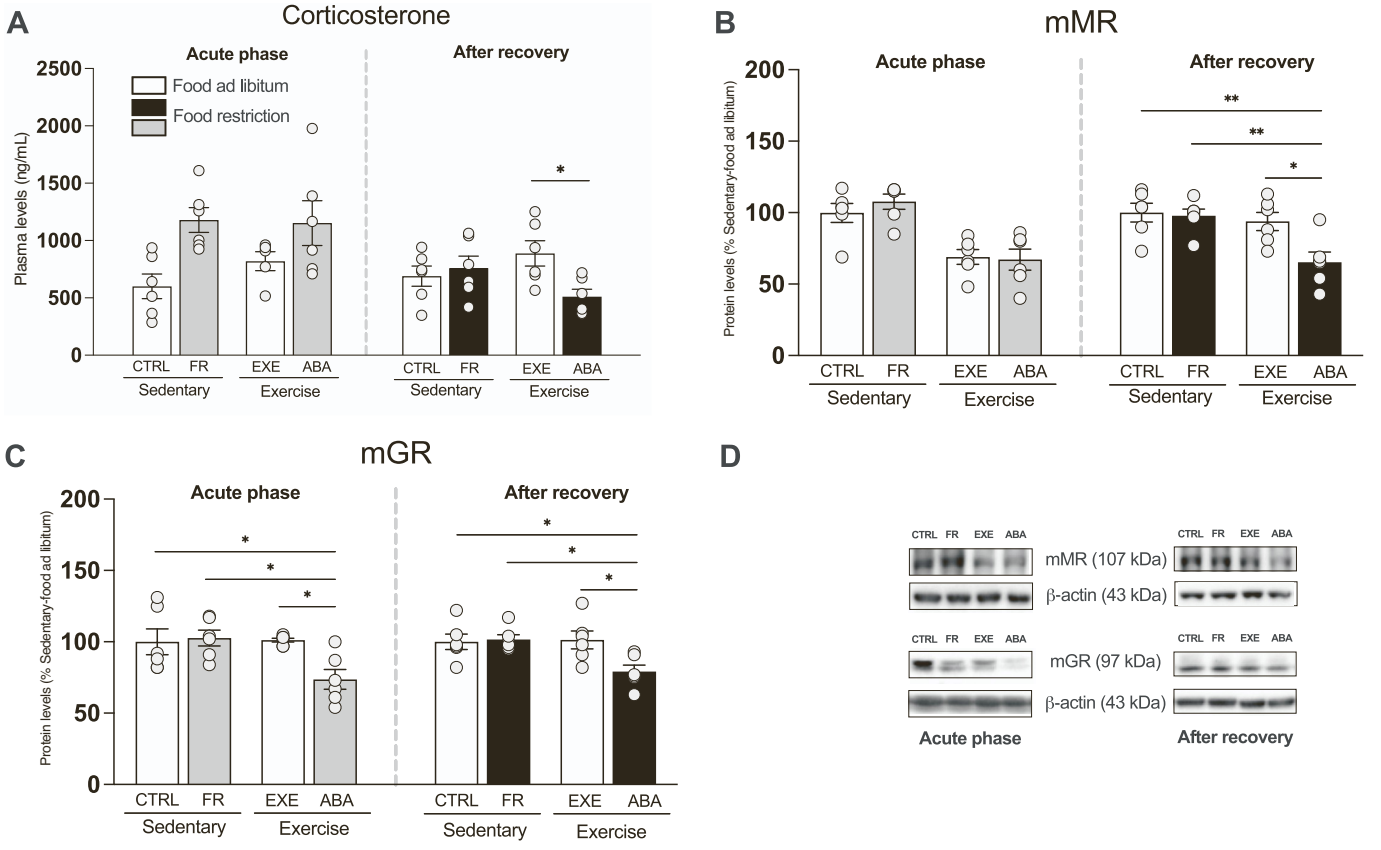

Fig. 2. Effect of the ABA induction on the circulating corticosterone levels and protein expression of membrane glucocorticoid receptors in the hippocampus. Panel (A) shows the levels of circulating corticosterone (CORT) measured in CTRL, FR, EXE and ABA rats in the acute phase of the phenotype (left) and after a period of body weight recovery (right). Data are expressed in ng/mL as the mean ± SEM of each group. As well, protein expression levels measured in the crude membrane fraction of the Hip of mGR are shown in panel (B) and mMR in panel (C). Representative immunoblots for each protein are shown in panel (D). Data are expressed in scatter plot bar graphs as percentages of sedentary-food ad libitum (CTRL) and represent the mean ± SEM. Two-way ANOVA followed by Tukey's multiple comparison test * $p < 0.05$, ** $p < 0.01$.
CTRL: control (n=6/time point); EXE: exercise (n=6/time point); FR: food restricted (n=6/time point); ABA: activity-based anorexia (n=6/time point).

2.4. Preparation of protein extracts and Western blot

Proteins from the homogenate and the crude synaptosomal fraction of the Hip were extracted, and Western Blot ran as previously described (Caffino et al., 2015). The conditions of the primary antibodies are reported in the supplementary materials.

Immunocomplexes were detected by chemiluminescence using Chemidoc MP Imaging System (Bio-Rad Laboratories, RRID: SCR_019037) and analyzed using the Image Lab software (Bio-Rad Laboratories). Gels were run two times each, and the results represent the average from two different runs. A correction factor was used to average different gels: correction factor gel B = average of (OD protein of interest/OD β-actin for each sample loaded in gel A)/(OD protein of interest/OD β-actin for the same sample loaded in gel B) (Mottarlini et al., 2022a; Caffino et al., 2020a). Full-size original cropped immunoblots related to the protein expression levels evaluated in the study are presented in supplementary figs. (1–4) and representative immunoblots for each protein are shown in Fig. 2D, 3E, 4E, 6D, 7L.

2.5. Corticosterone ELISA assay

After decapitation, plasma was prepared from trunk blood and CORT plasma levels were determined by ELISA assay (TECAN, Germany) as previously described (Caffino et al., 2020b).

2.6. Dendritic spine labeling and morphological classification

As described in the supplementary materials, tissue processing for dendritic spine analysis has been performed in CTRL and ABA rats at PND42 and PND49. Neuronal labeling and morphological classification of dendritic spines (as shown in Fig. 5E) in the whole Hip, primarily formed by pyramidal and granule cells, was achieved using the lipophilic membrane tracer 1,1'-Dioctadecyl- 3,3,3′,3'-Tetramethylindocarbocyanine Perchlorate (DilC18(3)) (Life Technologies cod. D282), as previously published (Caffino et al., 2018) and reported in the supplementary material, by a blinded operator. The number of neurons used for quantification was at least 25 for each experimental group (from each neuron, a different number of dendritic segments was analyzed); the neurons analyzed belonged to both hemispheres of the brain of n = 4/group/time point (8 hemispheres/group). The average dendritic length analyzed is 75 μm, and the length of the total dendrites analyzed was 2000 μm for each experimental group.

2.7. Spatial order object recognition (SOOR) test

As described in the supplementary materials, the SOOR task (Fig. 8E) has been performed in CTRL and ABA rats at PND42 and PND49 (Denninger et al., 2018). A total of 4 adolescent animals were removed from the study because they failed to successfully explore the objects (>10 s) during the sample phase. During the test phase, we measured the spatial discrimination index (DI), which was calculated as the difference in time spent by each animal exploring the object with a familiar location compared with the object with a novel location divided by the total time spent exploring both objects in the test period.

2.8. Statistics

Data were collected as independent determinations and are presented as means ± standard errors. Samples size was calculated using the software G*power 3.1.9.2 (http://gpower.hhu.de/) with an effect size = 0.4 (large, behavioral analysis), 0.25 (medium, molecular analysis), α error probability = 0.05, and power = 0.8.

Body weight, food intake, and wheel activity were analyzed by two-way analysis of variance (ANOVA) with repeated measures followed by Sidak multiple comparisons test.

CORT and protein levels changes, in which CTRL, FR, EXE, and ABA were considered, were analyzed by two-way ANOVA using food intake and physical activity as independent variables. When dictated by

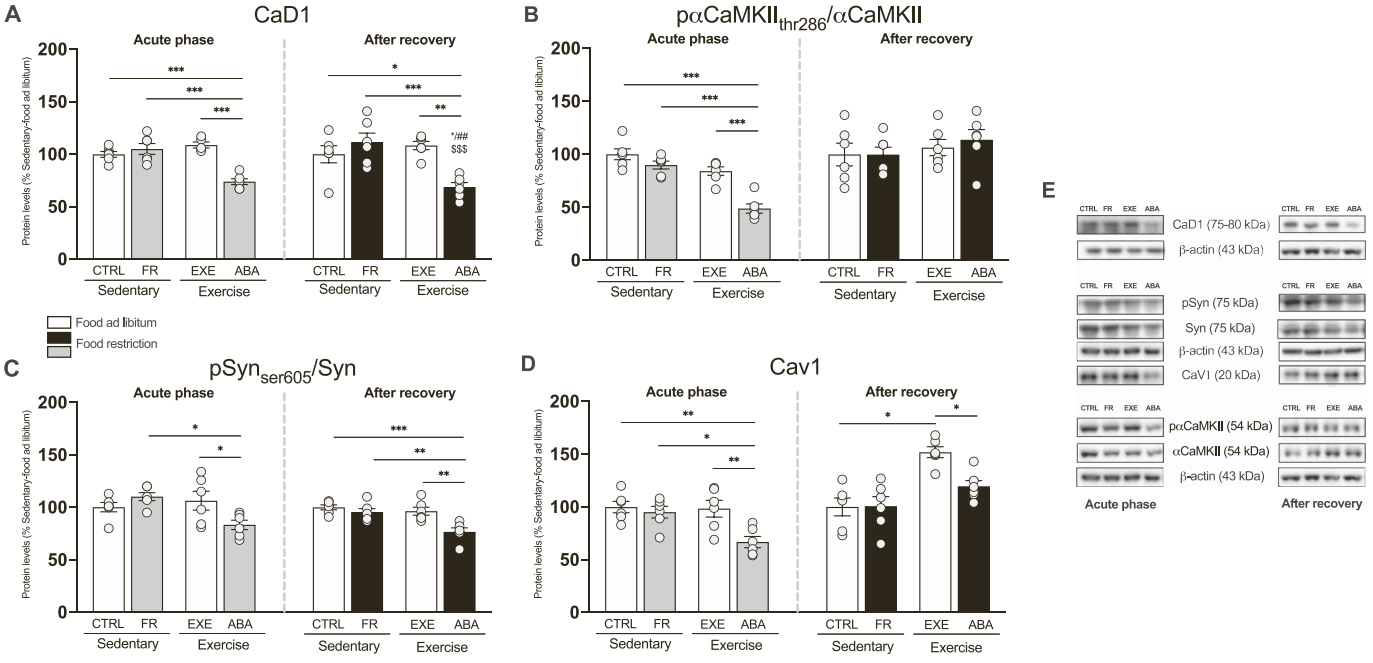

Fig. 3. Effect of the ABA induction on synaptic markers expression in the hippocampus. Protein levels of Caldesmon 1 (CaD1) (A) and levels of phosphorylation and total protein expression of αCaMKII represented as ratio of phospho(p)-αCaMKII in threonine (thr)286 over total αCaMKII (B). Levels of phosphorylation and total protein expression of Synapsin (Syn) represented as ratio of phospho(p)-Syn in serine (ser)605 over total Syn (C) and protein levels of caveolin 1 (Cav1) (D) were measured in CTRL, EXE, FR and ABA rats in the crude membrane fraction of the Hip, in the acute phase of the phenotype (left) and after a period of body weight recovery (right). Representative immunoblots for each protein are shown in panel (E). Data are expressed in scatter plot bar graphs as percentages of sedentary-food ad libitum (CTRL) and represent the mean ± SEM. Two-way ANOVA followed by Tukey's multiple comparison test * $p < 0.05$, ** $p < 0.01$, *** $p < 0.001$.
CTRL: control (n=6/time point); EXE: exercise (n=6/time point); FR: food restricted (n=6/time point); ABA: activity-based anorexia (n=6/time point).

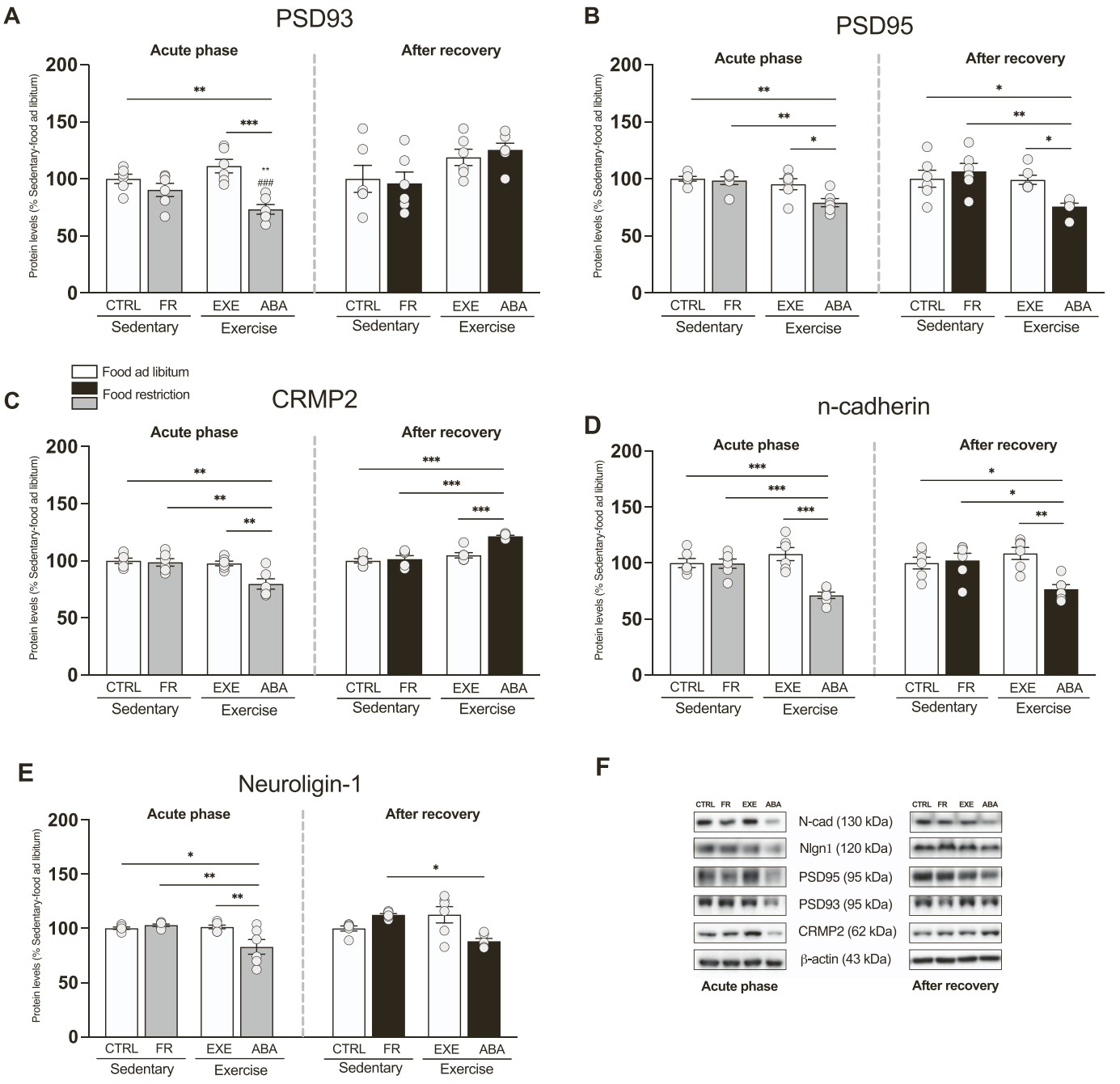

Fig. 4. Effect of the ABA induction on scaffolding and structural proteins in the hippocampus. Protein levels of the post synaptic density protein 93, PSD93 (A), post synaptic density protein 95, PSD95 (B) collapsin response mediator protein-2 (CRMP2) (C), n-cadherin (D), and of Neuroligin-1 (E) were measured in CTRL, EXE, FR and ABA rats in the crude membrane fraction of the Hip, in the acute phase of the phenotype (left) and after a period of body weight recovery (right). Representative immunoblots for each protein are shown in panel (F). Data are expressed in scatter plot bar graphs as percentages of sedentary-food ad libitum (CTRL) and represent the mean ± SEM. Two-way ANOVA followed by Tukey's multiple comparison test * $p < 0.05$, ** $p < 0.01$, *** $p < 0.001$.
CTRL: control (n=6/time point); EXE: exercise (n=6/time point); FR: food restricted (n=6/time point); ABA: activity-based anorexia (n=6/time point)

relevant interaction terms, Tukey's multiple comparisons test was used to characterize differences among individual groups of rats.

Changes in dendritic spine density and morphology and in protein levels (presented in Fig. 6–7) were tested for normality of residuals with the Kolmogorov-Smirnov test. Data with normal distribution were analyzed by unpaired Student's *t*-test (t). Data with a non-normal distribution were analyzed by the Mann-Whitney test (U). F and *p* values of independent variables of two-way ANOVA and t and p values of unpaired Student's t-test were reported in supplementary tables 1–3, 5–12, 14–15.

Pearson's product-moment coefficients (r) and linear regression analyses (R2) were calculated to study potential correlations between body weight and FAA (Supplementary Table 4).

Prism 8 (GraphPad Software Prism v8, San Diego, CA, USA) was used to analyze all data. Significance for all tests was assumed at $p < 0.05$.

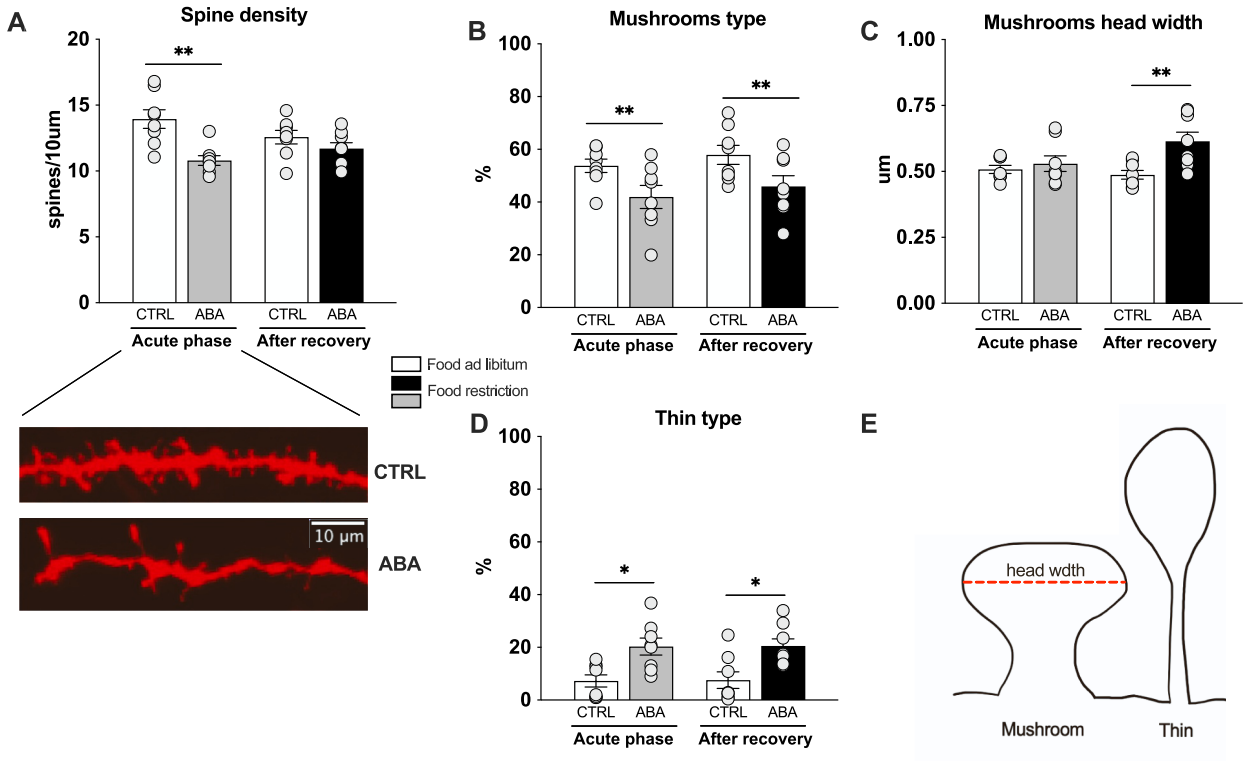

Fig. 5. Effect of ABA induction on dendritic spine density and morphology in the hippocampus. Panel (A) shows total spine density with representative images of dendrite segments from CTRL and ABA animals evaluated at PND42. Percentage of mushroom- and thin-shaped spines are shown in panel (B) and (D), respectively. Panel (C) show mushroom spines head width, and a schematic representation of mushroom- and thin-shaped spines is graphically represented in panel (E). $n > 2000$ spines from at least 25 different neurons for each group, around 5 dendritic segments for each hemisphere, 8 hemispheres/group. Data are presented in scatter plot bar graphs as the mean ± SEM in the acute phase of the phenotype (left) and after a period of body weight recovery (right). Two-way ANOVA followed by Tukey's multiple comparisons test * $p < 0.05$, ** $p < 0.01$ vs. CTRL-acute/recovery.
CTRL: control (n=8 hemispheres/time point); ABA: activity-based anorexia (n=8 hemispheres/time point).

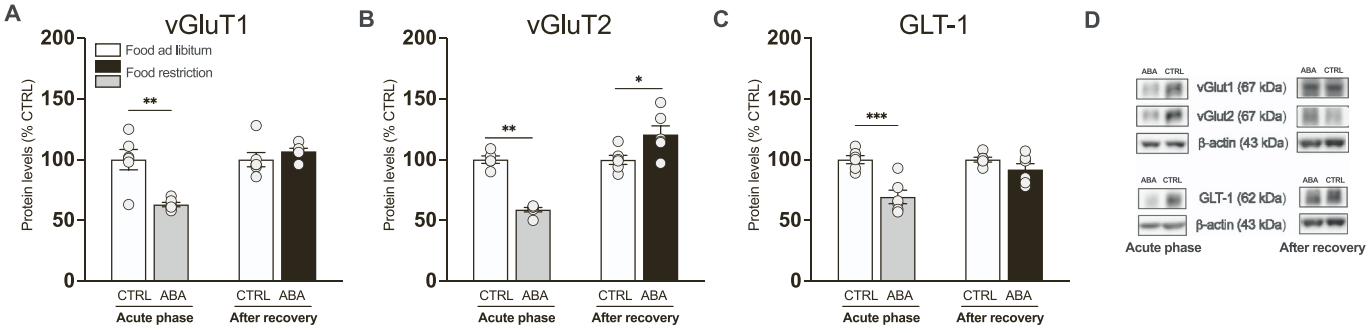

Fig. 6. Effects of the ABA protocol on glutamate transporters in the hippocampus. Protein levels of the vesicular glutamate transporter 1 (vGluT1) (A), vGluT2 (B) and of the glial glutamate transporter 1 (GLT-1) (C) were measured in CTRL and ABA rats in the crude membrane fraction of the Hip, in the acute phase of the phenotype (left) and after a period of body weight recovery (right). Representative immunoblots for each protein are shown in panel (D). Data are expressed in scatter plot bar graphs as percentages of sedentary-food ad libitum (CTRL) and represent the mean ± SEM. Unpaired Student's *t*-test * $p < 0.05$, ** $p < 0.01$, *** $p < 0.001$.
CTRL: control (n=6/time point); ABA: activity-based anorexia (n=6/time point).

3. Results

3.1. Behavioral readout of the ABA induction in adolescent female rats

In Fig. 1, panels B and D represent an over-day pattern plot of the running wheel activity (RWA) of EXE and ABA rats, respectively, measured at 30-min intervals. Qualitatively, our results show an increase of RWA in ABA rats right after 24 h from the beginning of the food restriction (PND39), while EXE animals did not. Moreover, EXE rats did not alter their physiologically balanced active/rest periods, whereas ABA rats constantly increased their activity over days, reducing their rest periods. To quantify these changes, we have first calculated the FAA, an index of hyperactivity that parallels the hyperactive symptoms in AN patients (Wu et al., 2014). ABA rats show a significant increase in FAA from PND40 to PND42 (Fig. 1C). Second, we confirmed that ABA rats travel a significantly higher total distance on the wheel (Fig. 1E), further strengthening the critical impact of food deprivation in exacerbating ABA running activity. Such behaviors induce a significant weight loss in ABA rats either with respect to CTRL, EXE and FR rats (Fig. 1F) despite ABA and FR rats eating the same amount of food during the restriction period (Fig. 1G). Interestingly, body weight negatively correlates with FAA only in ABA rats, as shown by the Pearson and linear regression

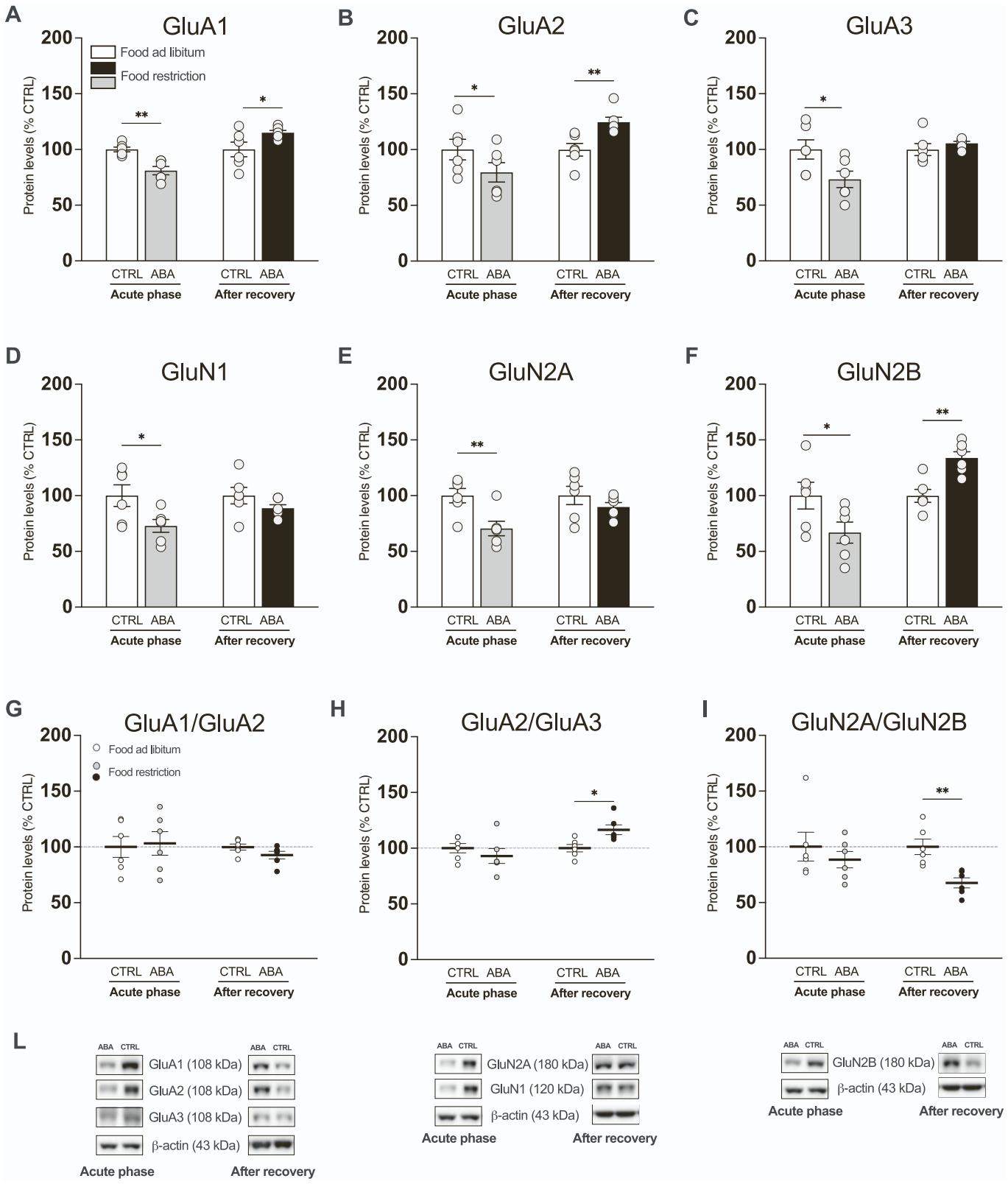

Fig. 7. Effects of the ABA protocol on the glutamatergic AMPA and NMDA receptors in the hippocampus. Protein levels of the GluA1 (A), GluA2 (B) and GluA3 (C) AMPA receptor subunits and of the GluN1 (D), GluN2A (E) and GluN2B (F) NMDA receptor subunits were measured in CTRL and ABA rats in the crude membrane fraction of the Hip, in the acute phase of the phenotype (left) and after a period of body weight recovery (right). GluA1/GluA2, GluA2/GluA3, and GluN2A/GluN2B ratios are presented in panels (G, H, I), respectively. Representative immunoblots for each protein are shown in panel (L). Data are expressed in scatter plot bar graphs as percentages of sedentary-food ad libitum (CTRL) and represent the mean ± SEM. Unpaired Student's t-test * $p < 0.05$, ** $p < 0.01$, *** $p < 0.001$.
CTRL: control (n=6/time point); ABA: activity-based anorexia (n=6/time point).

analyses as group mean (Fig. 1H) and as independent correlations (Fig. 1I, L). Throughout the refeeding period (PND42-PND49), ABA rats started recovering their weight, without however regaining that of CTRL animals at PND49 (Fig. 1F).

3.2. ABA induction dysregulates the non-genomic stress response and structural plasticity in the hip

Since circulating GCs regulate brain homeostasis (de Kloet and Joels, 2024) and hypercortisolemia are reported in adolescent AN patients (Luz Neto et al., 2019), we first measured plasma levels of CORT at both time points. In the acute phase, FR and ABA rats showed high levels of circulating CORT, an effect related to reduced food intake, whereas at PND49, CORT levels were reduced in ABA rats vs EXE rats (Fig. 2A).

In the Hip, we found a significant reduction of membrane MR (mMR) levels in both EXE and ABA rats, an effect may be due to the exercise condition. This effect persists even after body weight recovery only in ABA rats (Fig. 2B). Akin to mMR, the expression of mGR is significantly reduced in ABA rats both at the acute phase and even after refeeding (Fig. 2C). Indeed, no differences were present in mGR protein levels in animals exposed to FR or EXE only.

Interestingly, the ABA condition significantly reduces CaD1 protein levels at both time points (Fig. 3A) and the downstream pαCaMKII$_{Thr286}$/αCaMKII ratio, an indirect index of Ca^{2+}/CaM-dependent protein kinase II type α activation and involved in the structural stabilization of the synapse (Chapman and Stern, 1978), only at PND42 (Fig. 3B). Of note, we also observed that the pSyn1$_{Ser605}$/Syn1 ratio is increased in EXE animals while reduced in ABA rats, a reduction that persisted till PND49 (Fig. 3C). Also the levels of caveolin-1 (Cav1), a well-known scaffolding protein of lipid rafts and critically involved in synaptic vesicle exocytosis in hippocampal neurons (Koh et al., 2021), are significantly reduced in PND42 ABA rats; after recovery, Cav1 protein levels are restored compared to CTRL animals (Fig. 3D).

At structural level, the induction of the AN phenotype causes a significant reduction of both PSD93 (Fig. 4A) and PSD95 (Fig. 4B) protein levels, an effect that persists despite body-weight recovery for PSD95 (Fig. 4B), while PSD93 was still increased (Fig. 4A). Moreover, the protein levels of the Collapsin response mediator protein 2 (CRMP2), a microtubule-binding protein involved in cytoskeletal regulation, are reduced in ABA rats in the acute phase while enhanced following body-weight recovery (Fig. 4C). Looking for further insights into the synaptic contacts, we found that the protein levels of n-cadherin and neuroligin-1 were significantly reduced in ABA rats at both time points (Fig. 4D, E). Of note, no changes are present in the abovementioned targets, neither in FR nor in EXE groups. Thus, we focus our next analysis on the dendritic spine density and on the cognitive abilities only in ABA rats.

3.3. ABA induction alters dendritic spine density and the homeostasis of the glutamate synapse in the hip

The induction of the AN phenotype significantly reduced spine density (Fig. 5A), which was paralleled by a reduced percentage of mature active mushroom-shaped spines (Fig. 5B) in the acute phase. Of note, although the spine density was restored with the refeeding period (Fig. 5A), the reduction in mushroom-shaped spines persisted (Fig. 5B), together with a significant increase in the spine head width (Fig. 5C). Interestingly, in concomitance with the reduction in mushroom-shaped spines, we observed that the induction of the AN phenotype causes an increase at both time points of thin-shaped spines (Fig. 5D), the still immature type of spines, potentially prone to maturation.

Since such structural and morphological alterations influence the functionality of the glutamatergic synapse, we investigated whether the ABA condition would affect hippocampal glutamate homeostasis evaluating the contribution of the pre- and post-synaptic compartment and glial cells (the entire set of data on CTRL, FR, EXE and ABA are reported in supplementary table 13). At pre-synaptic level in PND42 ABA rats, we found down-regulation of vesicular glutamate transporter (vGluT)1 (Fig. 6A) and vGluT2 (Fig. 6B), which regulate glutamate release, and GLT-1, the glial glutamate transporter responsible for glutamate reuptake (Fig. 6C). After refeeding, vGluT2 was up-regulated, while no changes were observed either in vGluT1 or in GLT-1 (Fig. 6A-C). Moreover, at post-synaptic level, in the acute phase, ABA rats show an overall reduction in protein expression of the main AMPA receptor subunits GluA1, GluA2, and GluA3 (Fig. 7A-C), of the obligatory NMDA receptor subunit GluN1 and of GluN2A and GluN2B NMDA accessory subunits (Fig. 7D-F). Interestingly, after refeeding, ABA rats showed increased levels of GluA1, GluA2, and GluN2B (Fig. 7A, B, F), while no changes were observed for GluA3, GluN1, and GluN2A (Fig. 7C-E). Accordingly, we plotted data as ratio among subunits, as indices of specific subunit abundance, and receptor subunit composition. Although no changes in either AMPA and NMDA subunit ratios in the acute phase of the disorder were found (Fig. 7G-I), we observed a significant increase in the GluA2/GluA3 ratio (Fig. 7H), no changes in the GluA1/GluA2 ratio (Fig. 7G) and a decrease in the GluN2A/GluN2B ratio after recovery (Fig. 7I).

3.4. ABA induction alters the spatial memory in the SOOR test

Lastly, we wondered whether hippocampal-mediated cognitive abilities, such as spatial memory, could be affected in ABA rats. As shown in Fig. 8, CTRL and ABA rats show a similar time of exploration for the two objects in the training phase of the SOOR test, either at the acute phase (Fig. 8A) and after recovery (Fig. 8C). On the contrary, during the test phase, we observed that CTRL rats correctly identified the relocated object, exploring for more time the object displaced from the original position, as shown from the discrimination index either at PND42 or PND49. Conversely, ABA rats failed to correctly identify object displacement at both time points (Fig. 8B, D, F).

4. Discussion

In this study, we found a dysregulation of the mGR in the Hip of ABA rats that was paralleled by a reorganization of the hippocampal architecture and a redistribution of AMPA and NMDA receptors in the excitatory synapse. These data highlight a potential structural and molecular mechanism to explain the spatial memory deficits exhibited by ABA rats. Even though seven days of recovery restored body weight, morphological, structural and cognitive deficits still persisted. Our data contribute to explain, at least partially, the impact of the AN induction on the non-genomic response in the Hip, providing novel neurobiological basis for AN-induced long-lasting vulnerability.

In addition to the onset of the hyperactive phenotype typical of adolescent ABA female rats (Mottarlini et al., 2020; Mottarlini et al., 2022a; Mottarlini et al., 2022b; Milton et al., 2021; Collu et al., 2019), ABA rats displayed a marked disruption of circadian rhythms during the induction phase, widening their active phase even during the light period. This effect was paralleled by an increase in running activity during the two hours preceding feeding, measured as FAA activity, a readout of their increased motivation to engage in intense physical activity (Mistlberger, 1994). Since the FAA intensity became exponentially severe during the course of the experiment only in ABA rats, these data further corroborate the hypothesis that FAA is a direct consequence of starvation that, in turn, triggers body weight loss, as previously proposed (Tezenas du Montcel et al., 2023; Gabloffsky et al., 2022). In fact, FAA is considered as a main feature of hyperactivity in the ABA model and the hyperactive behavior of AN patients is associated with a longer hospitalization period (Solenberger, 2001) and poor treatment outcomes (Taranis and Meyer, 2011). Interestingly, alterations in the pattern of activity of ABA rats negatively correlated with body weight, further suggesting that disruption of the circadian rhythm in ABA rodents might be considered a maladaptive behavior predictive of a more severe phenotype. Wu and colleagues (Wu et al., 2014) observed that

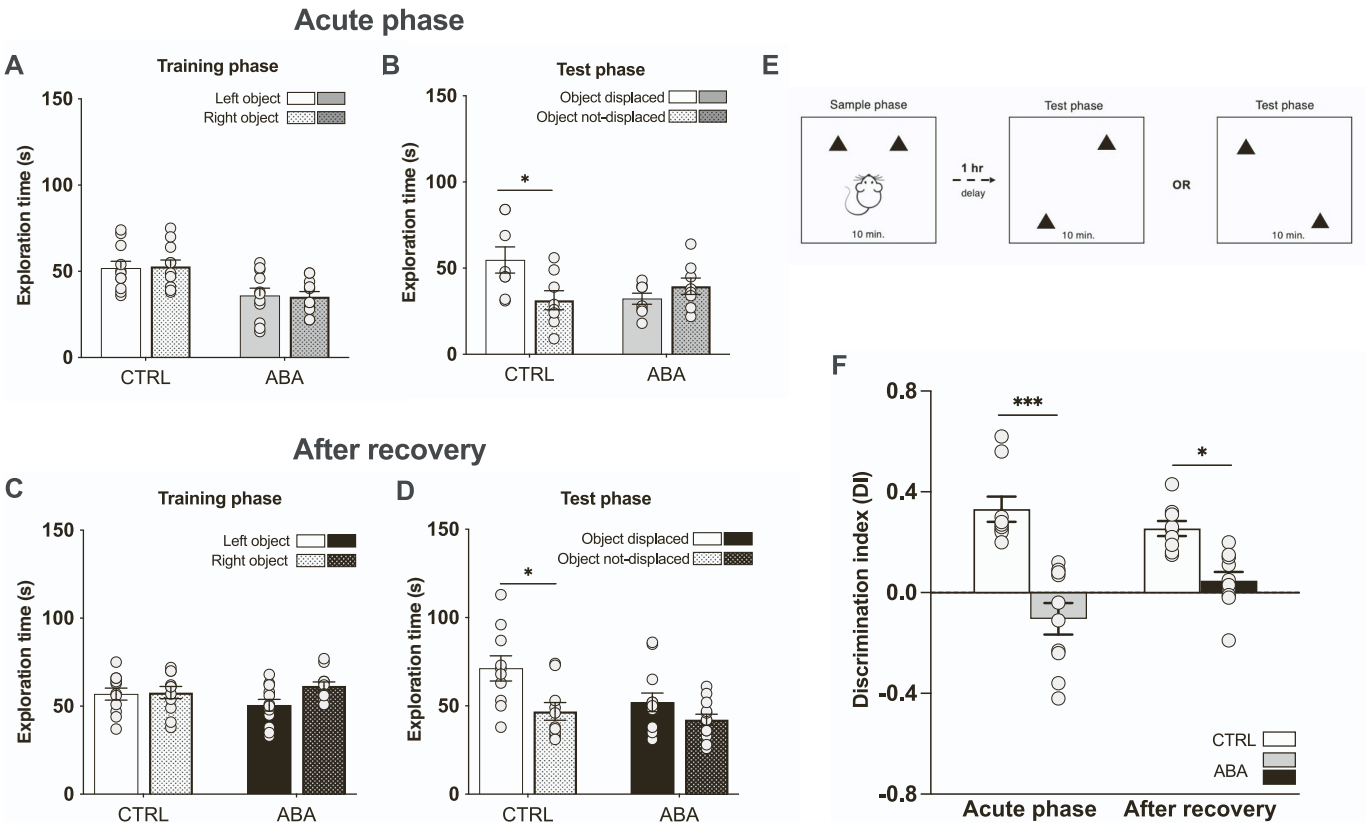

Fig. 8. Effect of the ABA induction on a spatial learning task performed in the acute phase of the phenotype and after a period of body weight recovery. Exploration time (*sec*) measured during the spatial order object recognition (SOOR) test in the training (A) and the test (B) phases in the acute phase, and after recovery (training C, test D) by CTRL and ABA rats. Spatial discrimination index, calculated for CTRL and ABA groups as (exploration time of object not displaced − exploration time of object displaced) / total time spent exploring both objects in the test phase, is presented in panel (F). A schematic representation of the SOOR test is shown in panel (E). Scatter plot bar graphs represent the exploration time (s) ± SEM, or the spatial discrimination index from at least six independent determinations for each experimental group. Two-way ANOVA followed by Tukey's multiple comparisons test * $p < 0.05$, ** $p < 0.01$ vs. CTRL-acute/recovery. CTRL = control ($n = 9$/time point); ABA = activity-based anorexia ($n = 10$/ time point).

FAA did not increase in highly susceptible ABA rats, clustered on the basis of the percentage of body weight loss. However, in our rat cohort, the correlation between increased FAA and body weight loss strongly suggests that, in adolescent female rats, FAA predicts a worse outcome: the age of animals used, young adult vs adolescent, and the length of the ABA protocol, 10 days of food restriction vs 4 days of food restriction, may account for the difference between the two studies. In particular, a strong inverse relationship between age and susceptibility has previously been observed in the ABA model (Gilman et al., 2019; Beeler et al., 2021; Aston et al., 2023) and AN patients (Grilo and Udo, 2021).

We also confirmed in our cohort of adolescent rats that CORT plasma levels were significantly elevated in ABA rats at PND42, as previously observed in adult ABA rats (Hillebrand et al., 2005; Boersma et al., 2016; Scherma et al., 2017) and in line with the elevation of cortisol levels found in AN patients (Thavarapatta et al., 2023). Interestingly, despite the rise in CORT levels seems to be due to food restriction per se, in the Hip mGR expression was reduced only in ABA rats, while mMR in both EXE and ABA rats, suggesting the involvement of the non-genomic stress response in the structural and functional alterations observed in the ABA model. Weight recovery influences hypercortisolemia by reducing CORT levels, suggesting that chronic HPA axis activation during the ABA induction may lead to compensatory and self-preserving HPA axis down-regulation (Agorastos and Chrousos, 2022). This transition from the hypercortisolemic state into hypocortisolemia may lead to a vulnerable phenotype with impaired GCs signaling and impaired stress reactivity; in line with this hypothesis, alterations in cortisol reactivity in the AN patients, elicited by an acute stressor, persisted even following BMI recovery (Schmalbach et al., 2021). At molecular level, we cannot discriminate whether the GCs preferentially affect mMR or mGR; however, since previous evidence demonstrate mMR contribution to the initial phase of the stress response, whereas mGR is involved in a second step (Joels et al., 2008; Dorey et al., 2011), we can hypothesize that the hyperstimulation of the HPA axis in ABA rats has led to rapid non-genomic effects involving both receptors at membrane levels. Of note, these alterations in the hippocampal mMR and mGR expression of ABA rats combined with reduced Cav1, essential for non-genomic action of GR (Samarasinghe et al., 2011), persist even when GCs levels are reduced and body weight is restored, thus accounting for a long-lasting dysregulation of the non-genomic GCs-responsive machinery.

Like exposure to repeated stress and excessive GCs (Liston and Gan, 2011; Borsini et al., 2023), we found that the ABA phenotype interferes with structural stability and destabilizes hippocampal dendritic spine density and shape. In fact, the persistent reduced expression of CaD1, a molecular link among GCs and dendritic spine development, suggests a destabilization of actin dynamics in dendritic spines via αCaMKII activity (Tanokashira et al., 2012; Fukumoto et al., 2009). In addition, N-cadherin and neuroligin-1 reductions, together with decreased pSyn I, might account for the detrimental effects of the ABA condition on dendritic spine loss, leading to a persistent destabilization of the hippocampal functionality. Of note, even though we cannot rule out the possibility that the reduction in these synaptic markers may account for reduced spine density, the structural reorganization of the hippocampal synapses destabilizes the post-synaptic terminal, as pointed by reduced PSD95, PSD93 and CRMP2 levels in the acute phase of the disorder. Remarkably, these molecular impairments were strengthened by reduced spine density and decreased number of mushroom-shaped

spines, along with an increased number of thin-shaped spines. Even though ABA rats display an increased formation of flexible thin spines, with a high capacity to expand their head and to mature in mushroom-shaped spines, this shift from mature to immature spine, which persisted even after weight recovery, is indicative of a reduction of synaptic contact and strength. This effect might contribute to explain the impaired spatial memory observed in ABA rats and AN patients (Rose et al., 2014; Stedal et al., 2022). Despite the reduction in PSD95 levels is maintained even following weight recovery, the rescue of PSD93 and the increase in CRMP2 levels paralleled by recovery of spine density and increased head width of mushroom-shaped spines reflect an adaptive mechanism to counteract the structural impairment induced by the ABA phenotype. However, this tentative rescue is not reflected at functional level since spatial memory is still impaired.

Since synaptic strength and the functional response of the synapses are strictly related to dendritic spine structure and the biochemical composition of the excitatory synapse at both pre- and post-synaptic levels (Bosch and Hayashi, 2012; Nakahata and Yasuda, 2018), our data demonstrate that the ABA-induced structural reorganization is paralleled by an overall reduction of glutamate transporters as well as of AMPA and NMDA receptor subunits at the achievement of the anorexic phenotype, further corroborating a depotentiation of synaptic strength in hippocampal excitatory synapses. Body weight recovery partially restores such AN-induced hypoglutamatergic state by increasing both GluA1 and GluA2 expression, enhancing the constitutive synaptic communication mediated by GluA2/GluA3 AMPA receptors and restoring GluN1 and GluN2A levels. However, the increased GluN2B levels, as well as the reduced GluN2A/GluN2B ratio, are indicative of maladaptive plasticity and heightened vulnerability as a consequence of an altered switch between GluN2B and GluN2A, previously observed as fundamental for the physiological maturation of synapses during brain development (Bellone and Nicoll, 2007; Liu et al., 2007).

5. Conclusion

This study provides the first evidence of the maladaptive effect of the ABA phenotype on the hippocampal non-genomic response of the HPA axis and in modulating the synaptic structure and composition of glutamate receptors. Such alterations might contribute to explain the spatial memory deficits observed following the induction of the anorexic phenotype at both time points. The lack of major changes in the abovementioned molecular targets of FR or EXE groups strengthens the strong impact of the ABA induction on hippocampal synaptic structural rearrangements.

We are aware that this study does not avoid limitations. First, only female rodents were used; in the literature, few studies investigated the impact of the ABA protocol on male rodents with conflicting results (Welch et al., 2018). Thus, further studies with a focused experimental paradigm are needed to compare males and females. Second, electrophysiological validation of hippocampal synaptic plasticity would narrow down some translational readouts. Third, we focused on the whole Hip, while analysis of the dorsal and ventral subregions, which modulate different functions, together with infralimbic and prelimbic cortices and amygdala, would be important. Last, since the genomic response of the GR system is involved in brain homeostasis modulation and in hippocampal-dependent spatial memory (Oitzl et al., 1997; Van Looveren et al., 2019), future investigations on the GR-induced translational response in AN are indeed required.

Funding sources

This research was supported by grants from MIUR PRIN (grant number: P2022E4MLS), Cariplo Foundation (2023−1003), Cariplo Foundation (grant number: 2017–0865), Nutricia Research Foundation (grant number: a2020-E3), Young IBRO Maternity/Parenthood Grant 2021 awarded to LC, as well as by grants from Nando and Elsa Peretti Foundation (grant number: 370) and Banca d'Italia, awarded to FF, and from MIUR Progetto Eccellenza 2023–2027.

Ethical statement

All animal procedures were conducted at the Department of Pharmacological and Biomolecular Sciences at the University of Milan and carried out following the principles set out in the following laws, regulations, and policies governing the care and use of laboratory animals: Italian Governing Law (D.lgs 26/2014; Authorization n.19/2008-A issued March 6, 2008, by Ministry of Health); the NIH Guide for the Care and Use of Laboratory Animals (Ed. 2011) and EU directives and guidelines (EEC Council Directive 2010/63/UE). Authorization for animal use has been obtained from the Italian Ministry of Health (#898–2016-PR). The experiments have been reported in compliance with the ARRIVE guidelines.

CRediT authorship contribution statement

Francesca Mottarlini: Writing – review & editing, Writing – original draft, Visualization, Methodology, Investigation, Formal analysis, Data curation, Conceptualization. **Giorgia Targa:** Writing – review & editing, Visualization, Validation, Software, Methodology, Formal analysis, Data curation, Conceptualization. **Beatrice Rizzi:** Writing – review & editing, Visualization, Validation, Methodology. **Fabio Fumagalli:** Writing – review & editing, Supervision, Funding acquisition, Conceptualization. **Lucia Caffino:** Writing – review & editing, Writing – original draft, Validation, Supervision, Project administration, Funding acquisition, Data curation, Conceptualization.

Declaration of Competing Interest

The authors declare no conflict of interest.

Data availability

Data will be made available on request.

Acknowledgements

The authors thank Giorgia Bottan, Benedetta Tarenzi and Fernando Castillo-Dìaz for participating in the initial phase of the work. Francesca Mottarlini is a recipient of a postdoc fellowship from the Zardi Gori Foundation. Beatrice Rizzi is supported by cycle XXXVIII of the PhD programme in Theoretical and Applied Neuroscience, DM351 (Finanziamenti PNRR).

Appendix A. Supplementary data

Supplementary data to this article can be found online at https://doi.org/10.1016/j.pnpbp.2024.111065.

References

Agorastos, A., Chrousos, G.P., 2022. The neuroendocrinology of stress: the stress-related continuum of chronic disease development. Mol. Psychiatry 27 (1), 502–513.

Aoki, C., Chowdhury, T.G., Wable, G.S., Chen, Y.W., 2017. Synaptic changes in the hippocampus of adolescent female rodents associated with resilience to anxiety and suppression of food restriction-evoked hyperactivity in an animal model for anorexia nervosa. Brain Res. 1654 (Pt B), 102–115.

Arango-Lievano, M., Borie, A.M., Dromard, Y., Murat, M., Desarmenien, M.G., Garabedian, M.J., et al., 2019. Persistence of learning-induced synapses depends on neurotrophic priming of glucocorticoid receptors. Proc. Natl. Acad. Sci. USA 116 (26), 13097–13106.

Arcelus, J., Mitchell, A.J., Wales, J., Nielsen, S., 2011. Mortality rates in patients with anorexia nervosa and other eating disorders. A meta-analysis of 36 studies. Arch. Gen. Psychiatry 68 (7), 724–731.

Aston, S.A., Caffo, B.S., Bhasin, H., Moran, T.H., Tamashiro, K.L., 2023. Timing matters: the contribution of running during different periods of the light/dark cycle to susceptibility to activity-based anorexia in rats. Physiol. Behav. 271, 114349.
Barbarich-Marsteller, N.C., 2013. Activity-based anorexia in the rat. In: Avena, N.M. (Ed.), Animal Models of Eating Disorders. Humana Press, Totowa, NJ, pp. 281–290.
Barker, G.R., Warburton, E.C., 2011. When is the hippocampus involved in recognition memory? J. Neurosci. 31 (29), 10721–10731.
Beeler, J.A., Mourra, D., Zanca, R.M., Kalmbach, A., Gellman, C., Klein, B.Y., et al., 2021. Vulnerable and resilient phenotypes in a mouse model of anorexia nervosa. Biol. Psychiatry 90 (12), 829–842.
Bellone, C., Nicoll, R.A., 2007. Rapid bidirectional switching of synaptic NMDA receptors. Neuron 55 (5), 779–785.
Bird, C.M., Burgess, N., 2008. The hippocampus and memory: insights from spatial processing. Nat. Rev. Neurosci. 9 (3), 182–194.
Boersma, G.J., Liang, N.C., Lee, R.S., Albertz, J.D., Kastelein, A., Moody, L.A., et al., 2016. Failure to upregulate Agrp and orexin in response to activity based anorexia in weight loss vulnerable rats characterized by passive stress coping and prenatal stress experience. Psychoneuroendocrinology 67, 171–181.
Borsini, A., Giacobbe, J., Mandal, G., Boldrini, M., 2023. Acute and long-term effects of adolescence stress exposure on rodent adult hippocampal neurogenesis, cognition, and behaviour. Mol. Psychiatr. 28 (10), 4124–4137.
Bosch, M., Hayashi, Y., 2012. Structural plasticity of dendritic spines. Curr. Opin. Neurobiol. 22 (3), 383–388.
Bou Khalil, R., Souaiby, L., Fares, N., 2017. The importance of the hypothalamo-pituitary-adrenal axis as a therapeutic target in anorexia nervosa. Physiol. Behav. 171, 13–20.
Caffino, L., Giannotti, G., Malpighi, C., Racagni, G., Fumagalli, F., 2015. Short-term withdrawal from developmental exposure to cocaine activates the glucocorticoid receptor and alters spine dynamics. Eur. Neuropsychopharmacol. 25 (10), 1832–1841.
Caffino, L., Messa, G., Fumagalli, F., 2018. A single cocaine administration alters dendritic spine morphology and impairs glutamate receptor synaptic retention in the medial prefrontal cortex of adolescent rats. Neuropharmacology 140, 209–216.
Caffino, L., Verheij, M.M.M., Roversi, K., Targa, G., Mottarlini, F., Popik, P., et al., 2020a. Hypersensitivity to amphetamine's psychomotor and reinforcing effects in serotonin transporter knockout rats: glutamate in the nucleus accumbens. Br. J. Pharmacol. 177 (19), 4532–4547.
Caffino, L., Mottarlini, F., Mingardi, J., Zita, G., Barbon, A., Fumagalli, F., 2020b. Anhedonic-like behavior and BDNF dysregulation following a single injection of cocaine during adolescence. Neuropharmacology 175, 108161.
Carrera, O., Fraga, A., Pellon, R., Gutierrez, E., 2014. Rodent model of activity-based anorexia. Curr. Protoc. Neurosci. 67, 9 47 1–11.
Chapman, R.H., Stern, J.M., 1978. Maternal stress and pituitary-adrenal manipulations during pregnancy in rats: effects on morphology and sexual behavior of male offspring. J. Comp. Physiol. Psychol. 92 (6), 1074–1083.
Chowdhury, T.G., Rios, M.B., Chan, T.E., Cassataro, D.S., Barbarich-Marsteller, N.C., Aoki, C., 2014a. Activity-based anorexia during adolescence disrupts normal development of the CA1 pyramidal cells in the ventral hippocampus of female rats. Hippocampus 24 (12), 1421–1429.
Chowdhury, T.G., Barbarich-Marsteller, N.C., Chan, T.E., Aoki, C., 2014b. Activity-based anorexia has differential effects on apical dendritic branching in dorsal and ventral hippocampal CA1. Brain Struct. Funct. 219 (6), 1935–1945.
Cole, A.B., Montgomery, K., Bale, T.L., Thompson, S.M., 2022. What the hippocampus tells the HPA axis: hippocampal output attenuates acute stress responses via disynaptic inhibition of CRF+ PVN neurons. Neurobiol Stress. 20, 100473.
Collantoni, E., Tenconi, E., Solmi, M., Meneguzzo, P., Marzola, E., D'Agata, F., et al., 2021. Hippocampal volumes in anorexia nervosa at different stages of the disorder. Eur. Eat. Disord. Rev. 29 (1), 112–122.
Collu, R., Scherma, M., Piscitelli, F., Giunti, E., Satta, V., Castelli, M.P., et al., 2019. Impaired brain endocannabinoid tone in the activity-based model of anorexia nervosa. Int. J. Eat. Disord. 52 (11), 1251–1262.
Connan, F., Lightman, S.L., Landau, S., Wheeler, M., Treasure, J., Campbell, I.C., 2007. An investigation of hypothalamic-pituitary-adrenal axis hyperactivity in anorexia nervosa: the role of CRH and AVP. J. Psychiatr. Res. 41 (1–2), 131–143.
de Kloet, E.R., Joels, M., 2024. The cortisol switch between vulnerability and resilience. Mol. Psychiatr. 29 (1), 20–34.
de Kloet, E.R., Joels, M., Holsboer, F., 2005. Stress and the brain: from adaptation to disease. Nat. Rev. Neurosci. 6 (6), 463–475.
Denninger, J.K., Smith, B.M., Kirby, E.D., 2018. Novel object recognition and object location behavioral testing in mice on a budget. J. Vis. Exp. 141.
Dorey, R., Pierard, C., Shinkaruk, S., Tronche, C., Chauveau, F., Baudonnat, M., et al., 2011. Membrane mineralocorticoid but not glucocorticoid receptors of the dorsal hippocampus mediate the rapid effects of corticosterone on memory retrieval. Neuropsychopharmacology 36 (13), 2639–2649.
DSM-V., 2013. Diagnostic and Statistical Manual of Mental Disorders: DSM-V, 5th ed. American Psychiatric Association, Washington DC.
Duclos, M., Gatti, C., Bessiere, B., Mormede, P., 2009. Tonic and phasic effects of corticosterone on food restriction-induced hyperactivity in rats. Psychoneuroendocrinology 34 (3), 436–445.
Foldi, C.J., Milton, L.K., Oldfield, B.J., 2017. The role of mesolimbic reward Neurocircuitry in prevention and Rescue of the Activity-Based Anorexia (ABA) phenotype in rats. Neuropsychopharmacology 42 (12), 2292–2300.
Frank, G.K.W., DeGuzman, M.C., Shott, M.E., Laudenslager, M.L., Rossi, B., Pryor, T., 2018. Association of Brain Reward Learning Response with Harm Avoidance, weight gain, and hypothalamic effective connectivity in adolescent anorexia nervosa. JAMA Psychiatry 75 (10), 1071–1080.
Fukumoto, K., Morita, T., Mayanagi, T., Tanokashira, D., Yoshida, T., Sakai, A., et al., 2009. Detrimental effects of glucocorticoids on neuronal migration during brain development. Mol. Psychiatry 14 (12), 1119–1131.
Gabloffsky, T., Gill, S., Staffeld, A., Salomon, R., Power Guerra, N., Joost, S., et al., 2022. Food restriction in mice induces food-anticipatory activity and circadian-rhythm-related activity changes. Nutrients 14 (24).
Gilman, T.L., Owens, W.A., George, C.M., Metzel, L., Vitela, M., Ferreira, L., et al., 2019. Age- and sex-specific plasticity in dopamine transporter function revealed by food restriction and exercise in a rat activity-based anorexia paradigm. J. Pharmacol. Exp. Ther. 371 (2), 268–277.
Grilo, C.M., Udo, T., 2021. Examining the significance of age of onset in persons with lifetime anorexia nervosa: comparing child, adolescent, and emerging adult onsets in nationally representative U.S. study. Int. J. Eat. Disord. 54 (9), 1632–1640.
Guinhut, M., Godart, N., Benadjaoud, M.A., Melchior, J.C., Hanachi, M., 2021. Five-year mortality of severely malnourished patients with chronic anorexia nervosa admitted to a medical unit. Acta Psychiatr. Scand. 143 (2), 130–140.
Hall, B.S., Moda, R.N., Liston, C., 2015. Glucocorticoid mechanisms of functional connectivity changes in stress-related neuropsychiatric disorders. Neurobiol Stress. 1, 174–183.
Hillebrand, J.J., van Elburg, A.A., Kas, M.J., van Engeland, H., Adan, R.A., 2005. Olanzapine reduces physical activity in rats exposed to activity-based anorexia: possible implications for treatment of anorexia nervosa? Biol. Psychiatry 58 (8), 651–657.
Ho, E.V., Klenotich, S.J., McMurray, M.S., Dulawa, S.C., 2016. Activity-based anorexia alters the expression of BDNF transcripts in the Mesocorticolimbic reward circuit. PLoS One 11 (11), e0166756.
Holland, J., Hall, N., Yeates, D.G., Goldacre, M., 2016. Trends in hospital admission rates for anorexia nervosa in Oxford (1968-2011) and England (1990-2011): database studies. J. R. Soc. Med. 109 (2), 59–66.
Iwajomo, T., Bondy, S.J., de Oliveira, C., Colton, P., Trottier, K., Kurdyak, P., 2021. Excess mortality associated with eating disorders: population-based cohort study. Br. J. Psychiatry 219 (3), 487–493.
Joels, M., Karst, H., DeRijk, R., de Kloet, E.R., 2008. The coming out of the brain mineralocorticoid receptor. Trends Neurosci. 31 (1), 1–7.
Kaye, W.H., Berrettini, W.H., Gwirtsman, H.E., Gold, P.W., George, D.T., Jimerson, D.C., et al., 1989. Contribution of CNS neuropeptide (NPY, CRH, and beta-endorphin) alterations to psychophysiological abnormalities in anorexia nervosa. Psychopharmacol. Bull. 25 (3), 433–438.
Kische, H., Ollmann, T.M., Voss, C., Hoyer, J., Ruckert, F., Pieper, L., et al., 2021. Associations of saliva cortisol and hair cortisol with generalized anxiety, social anxiety, and major depressive disorder: an epidemiological cohort study in adolescents and young adults. Psychoneuroendocrinology 126, 105167.
Koh, S., Lee, W., Park, S.M., Kim, S.H., 2021. Caveolin-1 deficiency impairs synaptic transmission in hippocampal neurons. Mol. Brain 14 (1), 53.
Lamanna, J., Sulpizio, S., Ferro, M., Martoni, R., Abutalebi, J., Malgaroli, A., 2019. Behavioral assessment of activity-based-anorexia: how cognition can become the drive wheel. Physiol. Behav. 202, 1–7.
Leuner, B., Shors, T.J., 2013. Stress, anxiety, and dendritic spines: what are the connections? Neuroscience 251, 108–119.
Licinio, J., Wong, M.L., Gold, P.W., 1996. The hypothalamic-pituitary-adrenal axis in anorexia nervosa. Psychiatry Res. 62 (1), 75–83.
Liston, C., Gan, W.B., 2011. Glucocorticoids are critical regulators of dendritic spine development and plasticity in vivo. Proc. Natl. Acad. Sci. USA 108 (38), 16074–16079.
Liu, Y., Wong, T.P., Aarts, M., Rooyakkers, A., Liu, L., Lai, T.W., et al., 2007. NMDA receptor subunits have differential roles in mediating excitotoxic neuronal death both in vitro and in vivo. J. Neurosci. 27 (11), 2846–2857.
Luz Neto, L.M.D., Vasconcelos, F.M.N., Silva, J.E.D., Pinto, T.C.C., Sougey, E.B., Ximenes, R.C.C., 2019. Differences in cortisol concentrations in adolescents with eating disorders: a systematic review. J. Pediatr. 95 (1), 18–26.
McEwen, B.S., Nasca, C., Gray, J.D., 2016. Stress effects on neuronal structure: Hippocampus, amygdala, and prefrontal cortex. Neuropsychopharmacology 41 (1), 3–23.
Meijer, O.C., Buurstede, J.C., Schaaf, M.J.M., 2019. Corticosteroid receptors in the brain: transcriptional mechanisms for specificity and context-dependent effects. Cell. Mol. Neurobiol. 39 (4), 539–549.
Mifsud, K.R., Reul, J., 2018. Mineralocorticoid and glucocorticoid receptor-mediated control of genomic responses to stress in the brain. Stress 21 (5), 389–402.
Milton, L.K., Mirabella, P.N., Greaves, E., Spanswick, D.C., van den Buuse, M., Oldfield, B.J., et al., 2021. Suppression of Corticostriatal circuit activity improves cognitive flexibility and prevents body weight loss in activity-based anorexia in rats. Biol. Psychiatr. 90 (12), 819–828.
Mistlberger, R.E., 1994. Circadian food-anticipatory activity: formal models and physiological mechanisms. Neurosci. Biobehav. Rev. 18 (2), 171–195.
Monteleone, P., Luisi, M., Colurcio, B., Casarosa, E., Monteleone, P., Ioime, R., et al., 2001. Plasma levels of neuroactive steroids are increased in untreated women with anorexia nervosa or bulimia nervosa. Psychosom. Med. 63 (1), 62–68.
Moschetta, M., Ravasenga, T., De Fusco, A., Maragliano, L., Aprile, D., Orlando, M., et al., 2022. Ca(2+) binding to synapsin I regulates resting ca(2+) and recovery from synaptic depression in nerve terminals. Cell. Mol. Life Sci. 79 (12), 600.
Mottarlini, F., Bottan, G., Tarenzi, B., Colciago, A., Fumagalli, F., Caffino, L., 2020. Activity-based anorexia dynamically dysregulates the glutamatergic synapse in the nucleus Accumbens of female adolescent rats. Nutrients 12 (12).
Mottarlini, F., Targa, G., Bottan, G., Tarenzi, B., Fumagalli, F., Caffino, L., 2022a. Cortical reorganization of the glutamate synapse in the activity-based anorexia rat model: impact on cognition. J. Neurochem. 161 (4), 350–365.

Mottarlini, F., Rizzi, B., Targa, G., Fumagalli, F., Caffino, L., 2022b. Long-lasting BDNF signaling alterations in the amygdala of adolescent female rats exposed to the activity-based anorexia model. Front. Behav. Neurosci. 16, 1087075.
Nakahata, Y., Yasuda, R., 2018. Plasticity of spine structure: local signaling, translation and cytoskeletal reorganization. Front Synaptic Neurosci. 10, 29.
Oitzl, M.S., de Kloet, E.R., Joels, M., Schmid, W., Cole, T.J., 1997. Spatial learning deficits in mice with a targeted glucocorticoid receptor gene disruption. Eur. J. Neurosci. 9 (11), 2284–2296.
Park, H.J., Lee, S., Jung, J.W., Kim, B.C., Ryu, J.H., Kim, D.H., 2015. Glucocorticoid- and long-term stress-induced aberrant synaptic plasticity are mediated by activation of the glucocorticoid receptor. Arch. Pharm. Res. 38 (6), 1204–1212.
Paxinos, G., Watson, C., 2013. The Rat Brain in Stereotaxic Coordinates, 7th Edition. 7th edition ed. Eselvier.
Petkova, H., Simic, M., Nicholls, D., Ford, T., Prina, A.M., Stuart, R., et al., 2019. Incidence of anorexia nervosa in young people in the UK and Ireland: a national surveillance study. BMJ Open 9 (10), e027339.
Reul, J.M., de Kloet, E.R., 1985. Two receptor systems for corticosterone in rat brain: microdistribution and differential occupation. Endocrinology 117 (6), 2505–2511.
Rose, M., Frampton, I.J., Lask, B., 2014. Central coherence, organizational strategy, and visuospatial memory in children and adolescents with anorexia nervosa. Appl. Neuropsychol. Child 3 (4), 284–296.
Samarasinghe, R.A., Di Maio, R., Volonte, D., Galbiati, F., Lewis, M., Romero, G., et al., 2011. Nongenomic glucocorticoid receptor action regulates gap junction intercellular communication and neural progenitor cell proliferation. Proc. Natl. Acad. Sci. USA 108 (40), 16657–16662.
Scherma, M., Satta, V., Collu, R., Boi, M.F., Usai, P., Fratta, W., et al., 2017. Cannabinoid CB1 /CB2 receptor agonists attenuate hyperactivity and body weight loss in a rat model of activity-based anorexia. Br. J. Pharmacol. 174 (16), 2682–2695.
Schmalbach, I., Herhaus, B., Passler, S., Runst, S., Berth, H., Wolff-Stephan, S., et al., 2021. Correction: cortisol reactivity in patients with anorexia nervosa after stress induction. Transl. Psychiatry 11 (1), 208.
Seed, J.A., McCue, P.M., Wesnes, K.A., Dahabra, S., Young, A.H., 2002. Basal activity of the HPA axis and cognitive function in anorexia nervosa. Int. J. Neuropsychopharmacol. 5 (1), 17–25.
Solenberger, S.E., 2001. Exercise and eating disorders: a 3-year inpatient hospital record analysis. Eat. Behav. 2 (2), 151–168.
Sousa-Lima, J., Moreira, P.S., Raposo-Lima, C., Sousa, N., Morgado, P., 2019. Relationship between obsessive compulsive disorder and cortisol: systematic review and meta-analysis. Eur. Neuropsychopharmacol. 29 (11), 1185–1198.
Stedal, K., Scherer, R., Touyz, S., Hay, P., Broomfield, C., 2022. Research review: neuropsychological functioning in young anorexia nervosa: a meta-analysis. J. Child Psychol. Psychiatry 63 (6), 616–625.
Sudhof, T.C., 2021. The cell biology of synapse formation. J. Cell Biol. 220 (7).
Swanson, A.M., Shapiro, L.P., Whyte, A.J., Gourley, S.L., 2013. Glucocorticoid receptor regulation of action selection and prefrontal cortical dendritic spines. Commun Integr Biol. 6 (6), e26068.
Tanokashira, D., Morita, T., Hayashi, K., Mayanagi, T., Fukumoto, K., Kubota, Y., et al., 2012. Glucocorticoid suppresses dendritic spine development mediated by down-regulation of caldesmon expression. J. Neurosci. 32 (42), 14583–14591.
Taranis, L., Meyer, C., 2011. Associations between specific components of compulsive exercise and eating-disordered cognitions and behaviors among young women. Int. J. Eat. Disord. 44 (5), 452–458.
Tezenas du Montcel, C., Cao, J., Mattioni, J., Hamelin, H., Lebrun, N., Ramoz, N., et al., 2023. Chronic food restriction in mice and increased systemic ghrelin induce preference for running wheel activity. Psychoneuroendocrinology 155, 106311.
Thavarapatta, S., Ungprasert, P., Witchel, S.F., Fazeli, P.K., 2023. Anorexia nervosa and adrenal hormones: a systematic review and meta-analysis. Eur. J. Endocrinol. 189 (3), S64–S73.
van Eeden, A.E., van Hoeken, D., Hoek, H.W., 2021. Incidence, prevalence and mortality of anorexia nervosa and bulimia nervosa. Curr. Opin. Psychiatry 34 (6), 515–524.
Van Looveren, K., Van Boxelaere, M., Callaerts-Vegh, Z., Libert, C., 2019. Cognitive dysfunction in mice lacking proper glucocorticoid receptor dimerization. PLoS One 14 (12), e0226753.
Walsh, B.T., Roose, S.P., Katz, J.L., Dyrenfurth, I., Wright, L., Vande Wiele, R., et al., 1987. Hypothalamic-pituitary-adrenal-cortical activity in anorexia nervosa and bulimia. Psychoneuroendocrinology 12 (2), 131–140.
Welch, A.C., Katzka, W.R., Dulawa, S.C., 2018. Assessing activity-based anorexia in mice. J. Vis. Exp. 135.
Won, S., Levy, J.M., Nicoll, R.A., Roche, K.W., 2017. MAGUKs: multifaceted synaptic organizers. Curr. Opin. Neurobiol. 43, 94–101.
Wu, H., van Kuyck, K., Tambuyzer, T., Luyten, L., Aerts, J.M., Nuttin, B., 2014. Rethinking food anticipatory activity in the activity-based anorexia rat model. Sci. Rep. 4, 3929.
Zajkowska, Z., Gullett, N., Walsh, A., Zonca, V., Pedersen, G.A., Souza, L., et al., 2022. Cortisol and development of depression in adolescence and young adulthood - a systematic review and meta-analysis. Psychoneuroendocrinology 136, 105625.
Zipfel, S., Giel, K.E., Bulik, C.M., Hay, P., Schmidt, U., 2015. Anorexia nervosa: aetiology, assessment, and treatment. Lancet Psychiatry 2 (12), 1099–1111.